Performance of a Reinforced Embankment on a Sensitive Soft Clay Foundation

A. Litwinowicz, C. V. Wijeyakulasuriya & A. N. Brandon
Queensland Transport, Queensland, Australia

ABSTRACT: The performance of a reinforced embankment constructed on soft clay is presented. The clay foundation and geosynthetic reinforcement (two types) were extensively instrumented to assess overall stability, the effect of reinforcement and monitor foundation movements. Observations at the end of fill placement are compared with traditional design techniques and the differences are discussed. Foundation consolidation during construction and mobilised fill strength are considered significant factors. Both reinforcements performed stiffer than index tests indicate. Finite element analyses using field derived parameters are compared with the observations. Long term monitoring indicates minimal decrease in reinforcement force.

1 INTRODUCTION

The performance of two types of reinforcement at the base of a bermed embankment (2.8 m total thickness) on a soft clay foundation is presented. The site is located on the Sunshine Motorway in South East Queensland, Australia. Observations from extensive instrumentation are compared with slip circle and plasticity solutions and the differences are discussed. The short term response of the reinforcements was stiffer than expected from index tests. Finite element modelling was performed and is compared with the observations. Monitoring of one reinforcement has been carried out for 590 days and the observed creep effects are briefly discussed.

2 SITE CHARACTERISTICS

This section of motorway traverses a swamp (0.3 m of standing water; surface RL 0.5 m) comprising coastal mangrove and tidal deposits of the holocene period. A 2 stage investigation comprised initial profiling of the soft clay with boreholes and cone penetrometers, and limited sampling (50 and 75 mm ϕ thin walled tubes). In the second stage, 100 mm ϕ piston samples were recovered and field shear vane tests were conducted in selected boreholes. Extensive Triaxial UU, CU and Oedometer tests were performed to assess strength and compressibility properties. The subsoil profile comprises dark grey to black, very soft/soft, organic marine silty clay ranging in depth from 4 - 10 m underlain by sandy deposits of the pleistocene period to RL -30 m. A typical profile of the soft clay is given in Figure 1. The sensitivity from the field vane is 3 - 4, which appears low compared to the liquidity indices in the top 5 m which are 1.5 - 2.5. Reliable evidence of a surface crust that could be adopted for design was not apparent. The vane gave a more consistent trend of S_u and formed the upper bound to the strength data. No strain softening

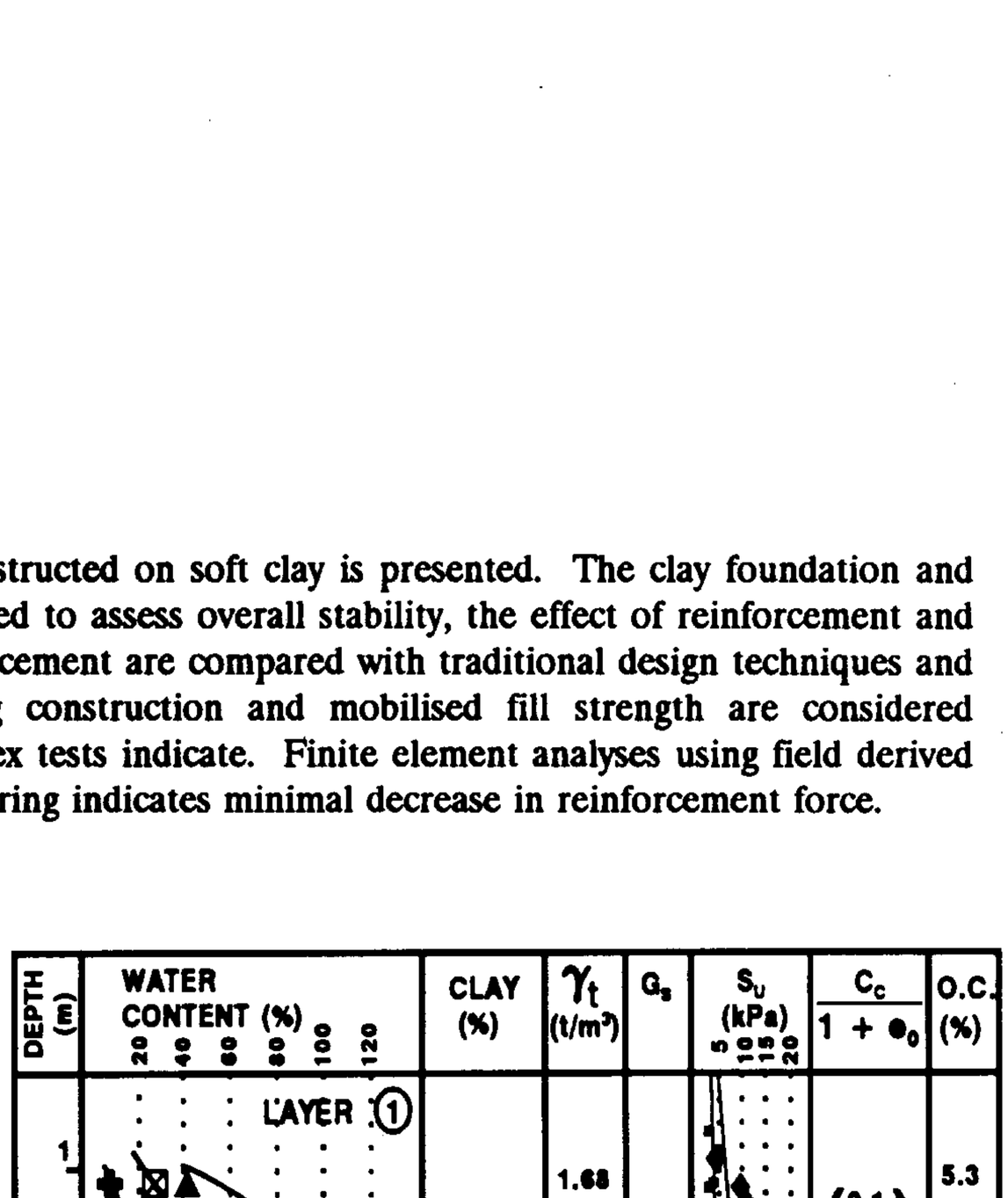

Fig.1 Geotechnical properties of the site

was observed in Triaxial UU tests (at a strain rate of 10%/hr) for axial strains >10%.

The soft clay deposit is lightly overconsolidated with an OCR of 2 - 3. Samples were carefully examined to identify macro-fabric details and drainage boundaries. Permeable seams were not apparent in continuous samples (except for slight sand traces near the top). This was confirmed by piezocone tests after embankment construction. A creep rate

of 2% strain per log cycle, in the normally consolidated stress range, was observed from laboratory tests. Given the sensitivity of the soft clays, compressibility parameters are likely to be underestimated in the normally consolidated range.

3 DESIGN METHODOLOGY

The embankment height of 2.6 m above natural ground could not be achieved in a single lift due to foundation instability. The need to raise the embankment to grade level in an overall construction period of 300 days led to the adoption of a bermed reinforced embankment with 2-stage construction.

Basal reinforcement improves embankment stability on soft ground by restricting lateral spreading of the fill, squeezing of the foundation (bearing failure) and rotational failure. The tensile stabilising force is generated in the reinforcement by shear stresses transmitted from the foundation and fill. The inward shear stress is limited by the reinforcement/soft clay bond and hence the soft clay S_u. The reinforcement must ensure a factor of safety (FOS) > 1 until the foundation has consolidated sufficiently to ensure stability unreinforced.

Total stress analyses, based on corrected vane S_u (Bjerrum, 1973), were used to assess the stability of the stage constructed embankment. A 2 layer stability model was adopted for the soft clay with the first 5 m assigned an S_u of 6 kPa, and a conservative S_u of 12 kPa thereafter. This approach was taken due to the uncertainty of Bjerrum's correction factor for organic soft clays. Due to the pessimistic S_u profile adopted, a marginal FOS was accepted subject to construction controlled by instrumentation and monitoring. Rotational stability was analysed using limit equilibrium with a computer implementation of Simplified Bishop's Slip Circle Method. Bearing failure was analysed with the lower bound plasticity method of Jewell (1988). Embankment batter slopes of 1V : 1.5H were adopted. The embankment was modelled as a granular material with $c' = 0$ - 10 kPa and $\phi' = 32°$.

The plasticity analyses considered squeezing beneath the batter slope/berm and indicated an FOS = 1 ($c'_{fill} = 0$) for a 2.6 m lift height above natural ground. The required reinforcement force, T_{req} was 60 kN/m (3 m from ℄) at an assumed tensile strain of 3-5%. Slip circle analyses gave an FOS of 1.3 ($c'_{fill} = 10$ kPa) with this T_{req}.

Two reinforcement types were used for construction and the reported properties (Exxon (1989), Netlon (1993)) from laboratory tests are given in Table 1. The polyester (PS) product has superior laboratory creep properties to the polypropylene (PP) e.g. at 30% of NBL the PS is creep insensitive whereas the strain in the PP increases 3 fold in 2 months of constant load. The PP reinforcement is manufactured from an extruded sheet which is punched and drawn. The PS reinforcement is comprised of strips 84 mm wide (180 mm pitch) with a polyester filament core sheathed in polyethylene.

4 INSTRUMENTATION DETAILS

The philosophy was to measure parameters to control stability, monitor foundation movements and determine long-term embankment behaviour. Comprehensive instrumentation allowed for redundancy and ensured that critical parameters could be assessed from multiple instruments to confirm the data. A typical instrumented cross-section (PP reinforcement) is shown in Figure 2. Lateral and vertical movements were

Table 1. Short term reinforcement properties (20°C)

Product	Polymer	Nominal Breaking Load (kN/m)	Strain at NBL (%)	$J_{sec3\%}$ (kN/m)
Tensar ER200	Polypropylene (PP)	200	8	3500
Paralink 200M	Polyester (PS)	200	12	2100

measured at various locations, and reinforcement performance was assessed by insitu measurement of force and strain from devices attached directly to the reinforcement.

Most instruments were installed after placement of a working platform and prior to laying of the reinforcement. The use of 7 mm screenings to cover the reinforcement provided interlock and is considered important to the successful functioning of each reinforcement and the force and strain measurement devices. Screenings were cleared to allow installation of the devices on the reinforcements. These devices incorporated vibrating wire transducers and were carefully calibrated.

4.1 Force and strain measurement

Force in a 1 m wide PP strip was measured with 3 load bolts, each of 4 tonne capacity. Clamps were designed to attach the bolts to the severed reinforcement so that twisting/bending effects were negated, the reinforcement wasn't damaged and slippage was eliminated. Laboratory proof testing was performed, and a small prestress was applied at installation to ensure sensitivity of the devices to loading. The PS material was instrumented with one load bolt at each of 6 locations using clamps specifically designed for the 84 mm wide strip.

Strains developed in both reinforcements were measured via strain gauges with a range of 25.4 mm extension, directly mounted with brackets (240 mm gauge length) designed to minimise bending and twisting effects. Gauges were installed after reinforcement tensioning during the placement of 7 mm

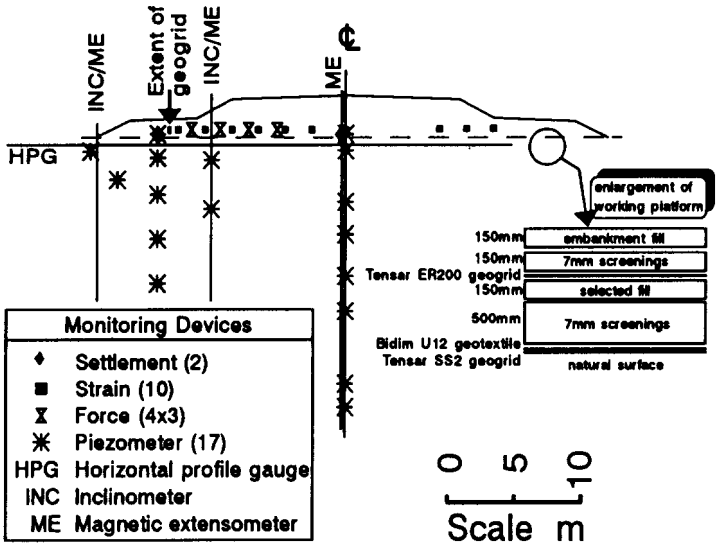

Fig.2 Instrumented section : PP reinforcement

screenings. Protective covers isolated the devices from the embankment material. Local compaction of fill adjacent to the gauges influenced the readings until placement of 0.5 m of material, and subsequent strain measurements have been corrected accordingly. At that time, the average load in the PP reinforcement was 0.4 kN. Average strains were also determined from lateral displacements measured using the inclinometer data, and extensometer magnets located on a horizontal profile gauge located below the PP reinforcement.

5 OBSERVATIONS OF FIELD PERFORMANCE

The construction history of both sections is shown in Figure 3. Although the absolute times differ, construction predominantly occurred over 20 days. Deformation profiles at the end of construction (EOC) are presented in Figure 4. Whilst the reinforced sections are within 20 m of each other and founded on the same soil deposit, the PS section has a slightly lesser clay thickness. Since the fill thicknesses applied are similar, the shorter drainage path has probably resulted in similar settlements being manifested. Lateral movements at the toe are higher for the PS section, probably due to increased consolidation and lower reinforcement stiffness.

5.1 Reinforcement strains

The ground temperature was ~15°C. Measured reinforcement strains are shown in Figures 5 and 6. The PS has strained significantly more than the PP, by a factor of up to 3 viz. ε_{max} for the PS of 1.65% compared with <0.5% for the PP. Both reinforcements show slight increases in strain for a short time after embankment completion. The strain profile at EOC across the embankment is shown in Figure 7. Both reinforcements display an ostensibly linear growth in strain from the edge reaching a maximum near ℄. For the PP reinforcement, the berm inclinometer and the horizontal profile gauge indicate the horizontal strain on, or in the vicinity of the reinforcement. These devices are in excellent agreement indicating 0.55% strain at the level of the profile gauge. At the level of the reinforcement the inclinometer indicates an average strain of 0.34% which is slightly higher than the strain gauge data. Construction equipment could however readily affect the inclinometer surface readings. It is considered that the strain measurements are valid and reasonably accurate, however the PP strain values are unexpectedly low.

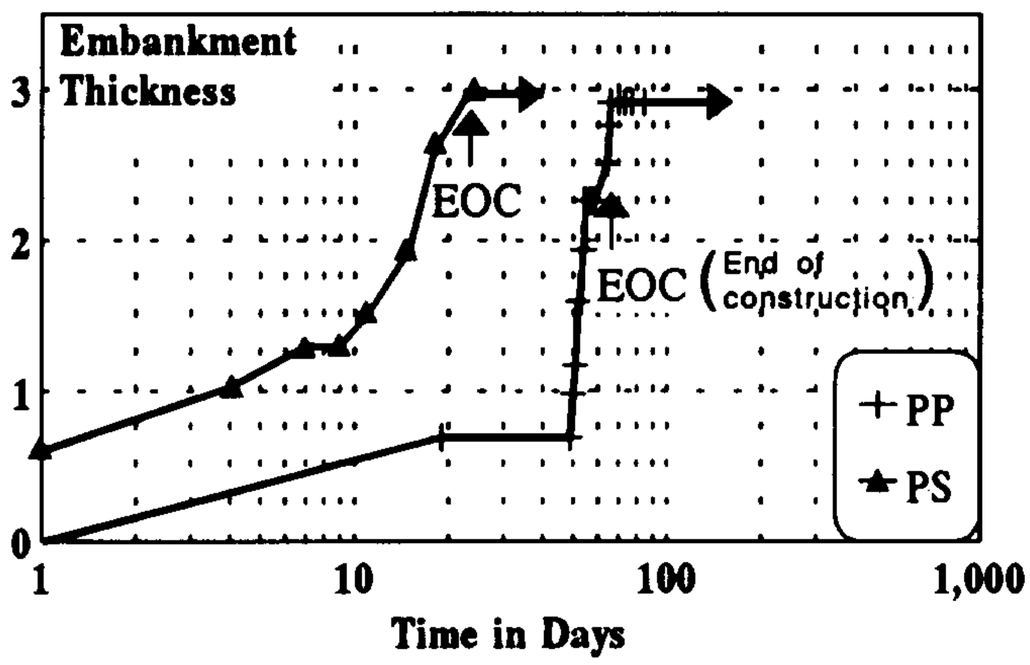

Fig. 3 Construction history

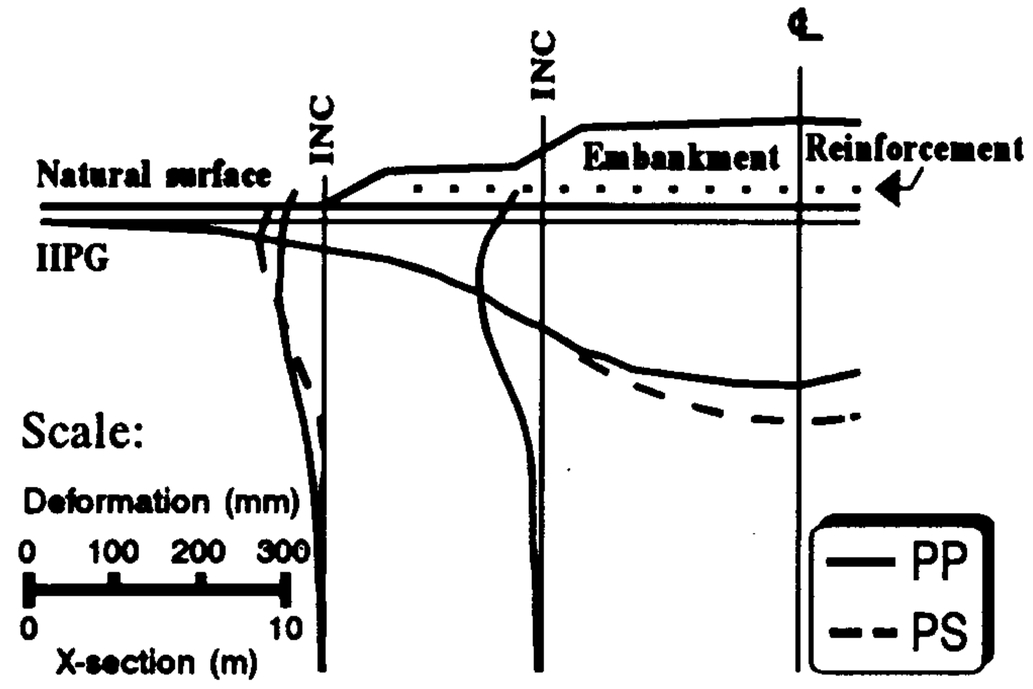

Fig. 4 Observed vertical and lateral deformations at EOC

5.2 Reinforcement forces

Measurements of force with time are depicted in Figures 5 and 6. Both reinforcements show a significant response during fill placement, and forces continue to increase slightly for a short period after EOC. The force profile (at EOC) is shown in Figure 7 and although the reinforcements behave comparably, their strain response is markedly different. Similar to the strain profile the forces increase towards ℄ and they appear to tend to zero some 2.5 m from the edge. The average J for the PP at EOC generally exceeds 7500 kN/m compared with $J_{sec\ 3\%}$ of 3500 from rapid laboratory tests. For the PS, J is 1800-3000 kN/m c.f. $J_{sec\ 3\%}$ = 2100 kN/m.

5.3 Comparison with Design Assumptions

Compared with T_{req} from the analyses in section 3, the mobilised forces for both reinforcements (T_{mob}) are less than half. There are numerous reasons for this, but the increase in foundation S_u due to partial consolidation and the contri-

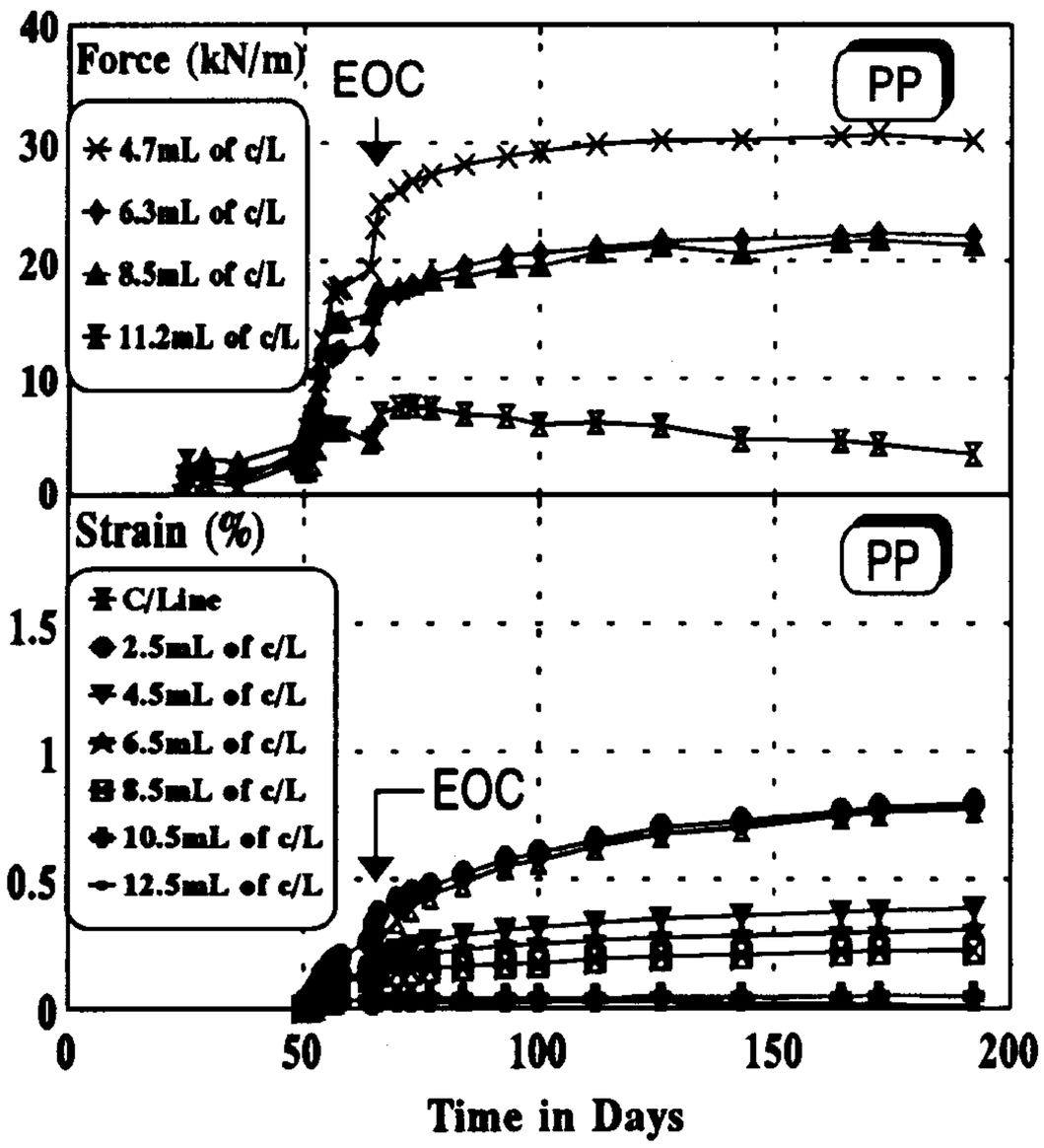

Fig. 5 Measured behaviour of PP reinforcement

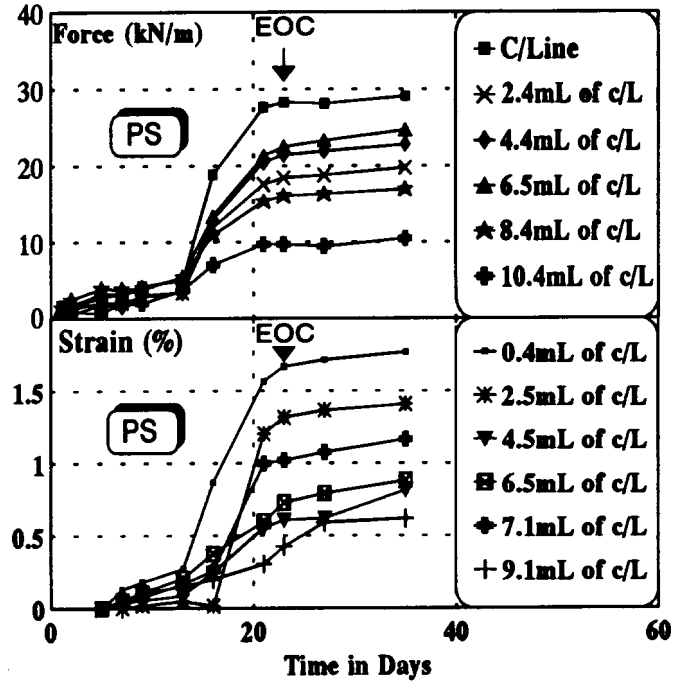

Fig. 6 Measured behaviour of PS reinforcement

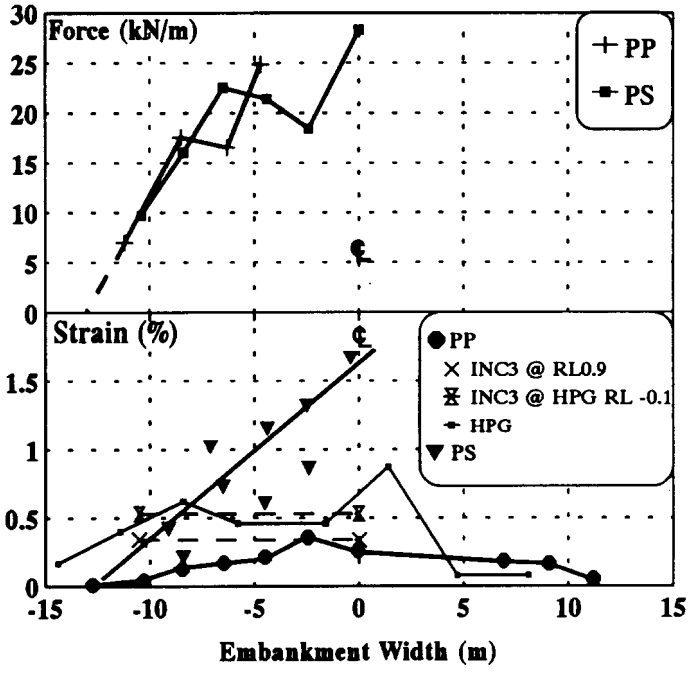

Fig. 7 Reinforcement force and strain profiles

bution of the fill strength are considered the most significant.

The fill strength for the design analyses was $c' = 10$ kPa and $\phi' = 32°$ intended to represent an essentially granular fill with a small pore suction. The fill actually used was a clay overburden which, in the compacted state exhibits an $S_u >> 50$ kPa and $c' = 35$ kPa, $\phi' = 20°$ from CU testing. The fill thrust to be resisted by the reinforcement in the plasticity solution would therefore be negligible, resulting in a significant decrease in the T_{req}. Similarly, slip circles would show a significant increase in FOS with such a fill strength. This is consistent with Shen (1989) who predicted that a decomposed granite mobilised a strength of some 50 kPa prior to failure of the Malaysian Trial Embankment.

The strain (ε_{req}) at which T_{req} would mobilise was subjectively chosen for design as 3% based on previous experiences with unreinforced embankments and the recommendations of Jewell (1988). The recommendation of Mylleville and Rowe (1991) of $\varepsilon_{req} < 0.5\%$ for brittle clays was considered too restrictive as this was based on undrained elastic-perfectly plastic analyses which may not be suited to partially drained construction on the soft clays at this site. Although not shown here, field vane testing after EOC indicated a 50% increase in S_u at the surface with minimal increase at 4m depth. This reduces the demand on the reinforcement by virtue of smaller lateral movements at the surface.

That the PS reinforcement developed similar forces to the PP punched and drawn sheet is of interest since the narrow PS strips provide <50% area coverage and do not have the potential for aperture-soil interlock nor passive resistance. It is considered that the granular working platform below, and the 150 mm of granular cover above the PS played a critical role in ensuring the bond necessary for the shear forces at the clay/platform and platform/fill interfaces to be effectively transferred to the embedded reinforcement, probably through concentration of shear stresses.

Although the plasticity solution is a lower bound, the embankment/foundation geometry and the S_u profile at this site results in a small improvement in stability between a perfectly smooth and fully rough interface. As the design exploits a rough interface, a significant T_{req} only gives a nominal improvement in FOS. It is feasible to have a safe embankment with small forces generated especially if partial drainage and fill strength (limited by the tensile strength) also contributed.

T_{req} was determined for squeezing of the clay beneath the batter slope and berm only. For fill with $\tau = 30$ kPa, and $c' = 0$ $\phi' = 32°$, the T_{req} beneath the batter point was 19 kN and 35 kN respectively which bounds the observed values.

6 FINITE ELEMENT ANALYSES

Numerical modelling was performed to compare current software and soil models with the observations and to model soil-structure interaction and compatibility at working conditions. The program CRISP (Britto and Gunn, 1987) was used in double precision in a plane strain analysis with 366 linear strain triangular elements. The foundation was treated as modified cam-clay, whilst the embankment was represented as an elastic-perfectly plastic material with a Mohr-Coulomb failure criterion ($\tau = 30$ kPa). Material properties (at EOC) are given in Table 2. The embankment construction (3 stages) closely followed the sequence for the PP section, each stage comprising 50 equal loading increments.

The reinforcement was modelled as a bar element with zero bending stiffness, $J = 7500$ kN/m, and was bounded by slip elements (Goodman et al, 1968). Slip occurred in accordance with a Mohr-Coulomb criterion with negligible movement until the interface shear strength was reached. The upper interface strength was set to the fill $\tau = 30$ kPa whilst the lower interface was set to the top of clay $S_u \approx 6$ kPa.

6.1 Derivation of parameters

Two sets of parameters were used for analysis. Although this is a Type C1 prediction (Lambe 1973) care was taken with the first data set (i) not to artificially "fit" parameters. λ was determined from extensometer measurements of foundation

strains for a small stress increment past the preconsolidation pressure. A field stress-strain curve for layer 2 is shown in Figure 8. κ was derived from 0.5 G_o, with G_o measured by seismic cone testing. The preconsolidation pressure was derived from the pore pressure response of the foundation on ℄ ($\Delta\sigma'_{vp}$ ≈ 22 kPa) and checked against extensometer stress-strain curves. Permeabilities were determined from the piezometer and strain response up to EOC. e_{cs} was determined from λ and κ given in Table 2. M was derived in accordance with Potts and Ganendra (1991) such that the plane strain analysis S_u (compression) approximated the vane S_u.

For the second data set (ii) the permeabilities were varied to closely fit the measured excess pore pressure isochrone at EOC (corrected for settlement). M was derived to approximate 0.8 times the vane S_u. The results of analyses using the measured PP stiffness are given in Figures 9 and 10.

Table 2. Soil properties for numerical modelling.

Layer		λ	κ	M	e_{cs}	υ'	k_H (m/s)	k_V (m/s)	γ (kN/m^3)
Clay	1	0.45	0.016	1.3	3.90	0.30	4.0E-8	4.0E-8	15.2
(i)	2	1.10	0.016	1.1	6.20	0.30	5.5E-9	5.5E-9	13.3
	3	0.50	0.016	1.2	3.70	0.30	1.0E-8	1.0E-8	15.7
Clay	1			1.25	3.92	0.35	5.0E-8	1.75E-8	
(ii)	2	"	"	0.60	6.50	0.35	3.0E-8	1.0E-8	
	3			0.81	3.70	0.25	1.5E-8	8.0E-9	

	E′(MPa)	υ'	τ (kPa)	γ (kN/m^3)
Embankment	25	0.25	30	20.0

(i) backanalysed (ii) fitted

6.2 Foundation deformations

Figure 9 shows that ℄ vertical displacements are overestimated by the FE analyses, mainly due to lower excess pore pressures for case (i). This improves for case (ii) as the isochrone is closely fitted. The lateral displacements are significantly underpredicted in the middle of the clay but the comparison improves near ground surface. Such analyses are renowned (Poulos 1972) for poor prediction of lateral movement mainly due to anisotropy, which is of concern when analysing reinforced embankments since such movements are fundamental to the reinforcement interaction. The steep gradient of lateral movement near ground surface indicates that the contribution of reinforcement is sensitive to location.

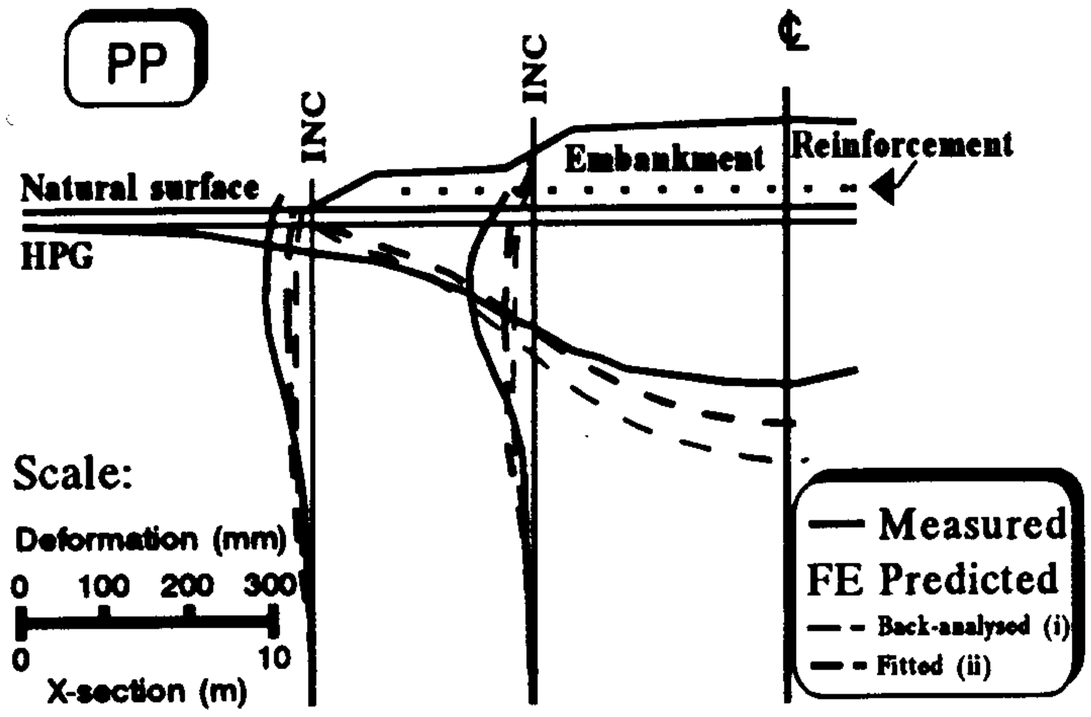

Fig. 9 Observed and F.E. predicted displacements.

6.3 Reinforcement forces

Predicted forces in Figure 10 are slightly lower than the observations as expected from the lateral displacement profiles. Although the reinforcement was modelled at ground surface, the PP reinforcement was placed ~0.3 m above. Given the steep gradient of the horizontal deformations at this level, lower forces might have been predicted if the reinforcement location was modelled exactly. The reinforcement location is important for analysis and construction since T_{mob} could be quite different if the location is raised by more than say 0.5 m.

A significant finding of the analyses is the force distribution and the prediction of negligible force ~2.5 m from the edge. Initially the reinforcement was modelled with J = 7500 kN/m, but compressive forces developed in the first two elements from the edge due to the stabilising berm. Subsequently these elements were assigned J = 0. This phenomenon also characterised the observations, which has implications on the extent of reinforcement for bermed embankments.

The analysis confirmed in principle the plasticity mechanism

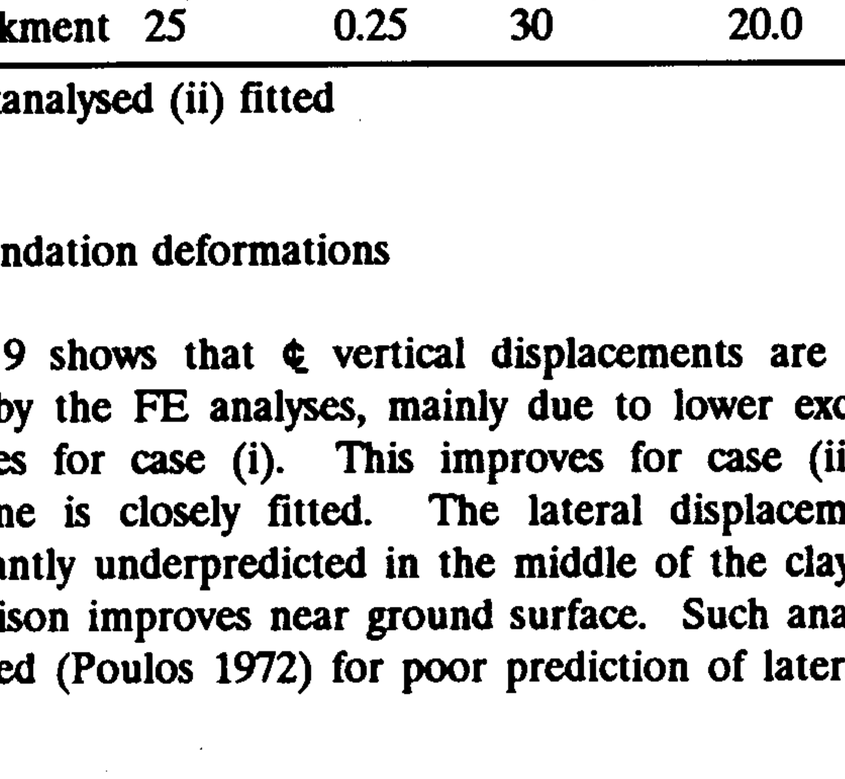

Fig. 8 Insitu stress-strain curve (Layer 2)

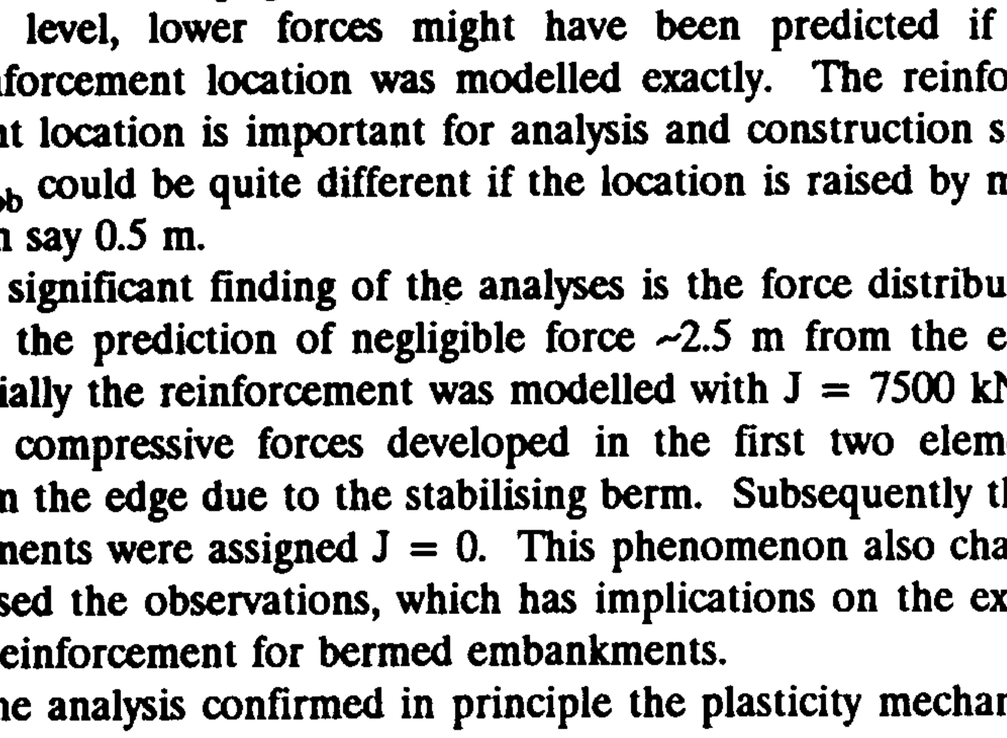

Fig. 10 Observed and F.E. predicted force profiles

of Jewell. A zone of contiguous plasticity developed virtually the full width of the embankment at a depth of 2.5-5 m. T_{mob} was contributed to by shear transmitted from both the fill and the foundation with average interface shear stresses (case (i)) of 3.5 kPa and 2.0 kPa respectively (maximum of 8.0 and 4.2 kPa). The fill has contributed significantly more than the clay foundation to T_{mob}, which is somewhat surprising given the strength of the fill. This has been observed in numerical analyses by Hird and Kwok (1990) who attribute this to bending of the fill layer and "arching". Furthermore, forces are seen to level off within 5 m of ℄.

6.4 Additional analyses

Analyses were performed with J = 0 to assess the effect of reinforcement. Reinforcement with J = 7500 kN/m (case (i)) results in 15% reduction in surface horizontal displacement. This contrasts the findings of Hird and Kwok who performed similar analyses (albeit undrained) for a 3 m high embankment with 6 m of clay which indicated up to 40% reduction. Such benefits should be considered with respect to partially drained behaviour and material properties.

Sensitivity analyses were performed to assess the effect of fill strength and stiffness. The maximum T_{mob} varied from 20.1 to 26.4 kN for E_{fill} of 10 to 100 MPa. Increasing the fill S_u from 30 to 50 kPa decreased T_{mob} by 9%, whilst a fill strength of $c' = 10$ kPa and $\phi' = 32°$ (design parameters) increased T_{mob} by 9%. Varying the stiffness parameters of the slip elements by a factor of 2 had minimal effect on T_{mob}.

Collapse of the embankment was modelled undrained (after EOC) by rapidly increasing the fill thickness and maintaining the original batter slope. The failure height for J = 7500 kN/m was ~4.3 m implying a factor of safety for the reinforced embankment of 1.48 c.f. design FOS of 1.0 - 1.3.

7 LONG TERM PERFORMANCE

The PP section has been monitored for 590 days. Maximum strains increased by ~0.5% from EOC to day 310; <0.1% was due to differential settlements, and the remainder caused by lateral foundation movements and creep effects. From isochronous creep curves, the maximum strain should be ~2.5% c.f. measured ε_{mob} of ~1.25%. Bassett (1986) also observed strains which were slightly lower than laboratory tests, and that the reinforcement continued to attract load with time at lesser strain rates. Strain/force development is complex for embankments which are consolidating and "confined" creep may be lower than index tests indicate. The effect of longer term creep will be reported when further data is to hand.

8 CONCLUDING REMARKS

Observations of an embankment with 2 reinforcement types indicated stiffness values higher than laboratory tests; this effect was more prominent for the PP reinforcement. The PS reinforcement developed similar forces, probably due to the strength and stiffness of the surrounding working platform.

T_{mob} was significantly less than indicated by limiting equilibrium and plasticity solutions, mainly due to foundation consolidation and probably higher fill strength contribution. Elasto-plastic Finite Element analyses gave force predictions of the right order but somewhat smaller lateral displacements. Positioning of the grid is important to the forces predicted. Sensitivity analyses indicated a smaller reduction in lateral displacements (with reinforcement) than suggested by published undrained analyses. FE analyses predicted that the edge portion of reinforcement beneath the berm would develop negligible force and this mirrored the observed behaviour.

Monitoring of the PP section for 590 days indicated strains significantly less than laboratory predictions. "Confined" creep requires further field measurements and assessment.

9 REFERENCES

Bassett, R.H. (1986) Presentation of instrumentation data, *Prediction Symp. on a Reinf. Emb. on Soft Ground (Stanstead Abbotts Bypass - Trial Emb.)*, Kings College, London.

Bjerrum, L. (1972) Embankments on soft ground, *Proc. ASCE Spec. Conf. on Earth and Earth-Supp. Struct., Purdue University,* Vol. II, 1-54.

Britto, A.M. and Gunn, M.J. (1987) *Critical state soil mechanics via finite elements,* 486 pp, Ellis Harwood, Chichester.

Exxon Chemical (1989). Geotextiles : Designing for soil reinforcement, Exxon Chemical Geopolymers Ltd, 1st Ed.

Goodman, R.E., Taylor, R.L. and Brekke, T.L. (1968) A model for the mechanics of jointed rock, *ASCE Journ. of the Soil Mech. and Found. Div.* V.94 (SM3) 637+

Hird, C.C. and Kwok, C.M. (1990) Parametric studies of the behaviour of a reinforced embankment, *4th Int. Conf. on Geotext., Geomemb. and Rel-Prod.,* The Hague, 137-142.

Jewell, R.A. (1988) The mechanics of reinforced embankments on soft soils, *Geotext. and Geomemb.,* 7 (4) 237-273.

Lambe, T.W. (1973) Predictions in soil engineering, *Geotechnique, 23,* (2) 149-202.

Mylleville, B.L.J. and Rowe, R.K. (1991) On the design of reinforced embankments on soft brittle clays, *Geotechnical Fabrics Report, May/June,* 12-24.

Netlon Limited (1993). Creep testing on "Tensar" ER200 geogrid at low stresses, Unpublished Report.

Potts, D.M. and Ganendra, D. (1991) Discussion on finite element analysis of the collapse of reinforced embankments on soft ground, *Geotechnique 41, (4),* 627-630.

Poulos, H.G. (1972) Difficulties in prediction of horizontal deformations of foundations, *Journ. of Soil Mech. & Found. Div.,* ASCE, Vol. 98, No. SM8, pp 843-848.

Shen, J.M. (1989) Prediction of trial embankment failure, *Proc. of Int. Symp. on Trial Embkts. on Malaysian Marine Clays,* Vol.2, 10.23.